DETERMINATION BY PHOTON CORRELATION SPECTROSCOPY OF PARTICLE SIZE DISTRIBUTIONS IN LIPID VESICLE SUSPENSIONS

JEFFREY H. GOLL AND GREGORY B. STOCK, *The Thomas C. Jenkins Department of Biophysics, The Johns Hopkins University, Baltimore, Maryland 21218 U.S.A.*

ABSTRACT A method of determining particle size distributions in lipid vesicle preparations is outlined. A vesicle suspension is modeled as a polydisperse mixture of spherical shells. The distribution of particle sizes in this mixture is approximated by a continuous, piecewise linear function called a first-order spline. Excellent simultaneous fits to photon correlation spectroscopy data gathered at several different angles are presented. An error analysis is included to indicate the resolution of the method.

INTRODUCTION

Photon correlation spectroscopy (PCS) is widely used to determine the sizes of particles in solution (1, 2). Considerable difficulties have arisen, however, in the interpretation of PCS experiments performed on polydisperse solutions. Several methods have been devised to attempt to cope with polydispersity. The method of cumulants (3, 4) yields several moments of a particle size distribution. The method is limited, however, since all the moments must be known to characterize a distribution uniquely, and only the first two are generally determined with adequate accuracy (3). When it is possible to make reasonable assumptions about the nature of the distribution, a more complete characterization can be obtained. Thus Bargeron (5) assumed a Gaussian particle size distribution and used the first two cumulants calculated from PCS data to determine the best-fit Gaussian distribution for polystyrene latex spheres. Aragon and Pecora (6) gave analytic expressions for the correlation function arising from a Schulz distribution. They suggest using their results in fitting data gathered with scattering samples such as solutions of phospholipid vesicles. Stock (7) has extracted bacterial swimming speed distributions from PCS data. He modeled the distribution as a continuous, piecewise linear function called a first-order spline and used a nonlinear least squares algorithm to find the best-fitting distribution of the assumed form. Except when constraints are deliberately imposed, the form of the distribution is relatively unrestricted with this method.

Dr. Goll's current address is: P.O. Box 5936, M.S. 134, Texas Instruments, Inc., Dallas, Tex. 75222

In this paper it is shown that particle size distributions of solutions of phospholipid vesicles can be extracted from PCS data by modeling the distribution as a first-order spline function. It is shown that a single distribution function gives excellent fits to PCS data gathered at several different scattering angles.

METHODS

Data Fitting

In a digital homodyne PCS experiment, $g^{(2)}(\tau, \theta)$, the normalized autocorrelation function of the intensity scattered at the angle θ, can be measured. Assuming that the scattered **E** field amplitude is Gaussian random-distributed, the Siegert relation (8) may be used to obtain an experimental estimate of the normalized field autocorrelation function, $|g^{(1)}(\tau, \theta)|$, from $g^{(2)}(\tau, \theta)$. This estimate may be compared with the theoretical $|g^{(1)}_{\text{theory}}(\tau, \theta)|$ predicted for any population of scattering particles.

The phospholipid vesicle solution is modeled here as a polydisperse population of spherical shells of wall thickness 40 Å. The size distribution is described by a first-order spline. The distribution function most consistent with the autocorrelation data is obtained by least squares fitting techniques (9), using as variables the parameters which define the spline. For this model the predicted field autocorrelation function is,

$$|g^{(1)}_{\text{theory}}(\tau, \theta)| = \int_0^\infty dR\{N(R)I(R, \theta) \exp[-D(R)q^2(\theta)\tau]\} / \int_0^\infty dR\{N(R)I(R, \theta)\}. \quad (1)$$

Here q is the magnitude of the scattering vector (1). $D(R)$ is the diffusion coefficient of a vesicle of radius R. Assuming that the vesicles diffuse as hard spheres, we may evaluate $D(R)$ by Stokes's law (10). $I(R, \theta)$, the intensity scattered in the direction of θ by a single particle of outer radius R, is given by:

$$I(R, \theta) = C\left(\tfrac{4}{3}\pi R^3\right)^2 P(R, \theta), \quad (2)$$

where C is a constant involving the polarizability of the particle (assumed uniform in the lipid region of a vesicle) and $P(R, \theta)$ is given by the Rayleigh-Gans form factor for spherical shells (11):

$$P(R, \theta) = (3/qR)^6\{[\sin(qR) - qR\cos(qR)] - [\sin(qR_i) - qR_i\cos(qR_i)]\}^2. \quad (3)$$

Here R and R_i are the radii of the outer and inner walls of the vesicle. Finally, $N(R)$ is the particle number density function.

The first-order spline used to approximate $N(R)$ is a bounded, continuous, piecewise-linear function. It is defined in terms of a selected set of radii $\{R_0, R_1, \ldots, R_k\}$ called junction points, or knots. R_k and R_0 are upper and lower bounds on the allowed particle sizes: $N(R) = 0$ for $R \geq R_k$ and $R \leq R_0$. $N(R)$ is linear over all intervals $[R_j, R_{j+1}]$, $j = 0, 1, \ldots k - 1$. Thus $N(R)$ is completely determined by the set of values $\{N(R_l) \mid l = 1, 2, \ldots k - 1\}$. The distribution in this form is a first-order spline (7, 12). It is possible to use higher (m^{th}) order splines to approximate the distribution by "smoother" functions which are m^{th} order polynomials on the intervals $[R_j, R_{j+1}]$ and which have $m - 1$ derivatives which are continuous everywhere. This extension will not be used here.

Any linear spline with knots at $\{R_0, R_1, \ldots, R_k\}$ may be written as a linear combination of

basis functions $\Delta_1(R; R_i, R_{i+1}, R_{i+2})$:

$$N(R) = \sum_{i=0}^{k-2} n_i \Delta_1(R; R_i, R_{i+1}, R_{i+2}) \tag{4}$$

Stock (7) describes these basis functions in detail.

Combining Eqs. 1–4 yields:

$$|g^{(1)}_{\text{theory}}(\tau, \theta)|$$

$$= \frac{\sum_{i=0}^{k-2} n_i \int_{R_i}^{R_{i+2}} dR\{R^6 P(R, \theta)\Delta_1(R; R_i, R_{i+1}, R_{i+2}) \exp[-D(R)q^2(\theta)\tau]\}}{\sum_{i=0}^{k-2} n_i \int_{R_i}^{R_{i+2}} dR\{R^6 P(R, \theta)\Delta_1(R; R_i, R_{i+1}, R_{i+2})\}}, \tag{5}$$

The integrals in Eq. 5 involve slowly varying functions of R and are readily evaluated by numerical integration, leading to:

$$|g^{(1)}_{\text{theory}}(\tau, \theta)| = \sum_{i=0}^{k-2} n_i T_i(\tau, \theta) \Big/ \sum_{j=0}^{k-2} n_j B_j(\theta). \tag{6}$$

Only $k - 2$ of the $k - 1$ variables n_i are independent, since $|g^{(1)}_{\text{theory}}(\tau, \theta)|$ depends only on relative particle numbers. The dependent variable may be eliminated by setting the donominator of Eq. 6 equal to a constant and then solving for one of the coefficients—e.g. n_{k-2}. (This corresponds to supposing that the unknown total intensity scattered in the direction θ takes a given value.) The expression for $|g^{(1)}_{\text{theory}}(\tau, \theta)|$ is then linear in the parameters $\{n_i \mid i = 0, 1, \ldots, k - 3\}$ and a linear least squares technique (9) may be used to extract from PCS data the best-fit $N(R)$. It is not possible with this linear technique to restrict $N(R)$ to physically meaningful (nonnegative) values, as was demonstrated by a trial case that gave a best-fit $N(R)$ with regions having negative numbers of particles. To avoid this difficulty, fitting was based on a nonlinear least squares algorithm (9, 13).

In the nonlinear technique $N(R)$ is restricted to nonnegative values by replacing Eq. 4 by:

$$N(R) = \sum_{i=0}^{k-2} s_i^2 \Delta_1(R; R_i, R_{i+1}, R_{i+2}), \tag{7}$$

so that

$$|g^{(1)}_{\text{theory}}(\tau, \theta)| = \sum_{i=0}^{k-2} s_i^2 T_i(\tau, \theta) \Big/ \sum_{j=0}^{k-2} s_j^2 B_j(\theta), \tag{8}$$

and using the s_i as the variables in the fitting procedure. (Thus $s_i^2 = n_i$.) Any first-order spline that is everywhere nonnegative can be represented in the form of Eq. 7. The nonlinear technique also makes possible the *simultaneous* fitting of data taken at several different scattering angles with a single parameterized $N(R)$. Simultaneous fitting provides a more stringent test of the validity of the model used to describe the scattering population. The dependent para-

meter in the set $\{s_i\}$ is removed in the nonlinear scheme by simply fixing the value of one parameter, s_f. To simplify the computations, the instrumental constants (amplitudes) associated with data gathered at the various angles are evaluated by cumulant analysis.

Data Collection

Prescaled intensity autocorrelation functions were obtained with a serial digital autocorrelator[1] interfaced with a Nova 2 minicomputer (Data General Corp., Southboro, Mass.) and an optical arrangement described previously (14). Sample preparation is described elsewhere.[2] For each θ, autocorrelation data were gathered during many equal and consecutive short ($\sim$1 s) periods of time. The final $g^{(2)}(\tau, \theta)$ was an average of the results of selected short experiments. Short experiments were included in the average if their calculated theoretical backgrounds fell within a preselected number ($\sim$1) of standard deviations of the mean background. The selected short experiments were also used in calculating the standard deviations associated with $g^{(2)}(\tau, \theta)$. This procedure had several desirable consequences. Data accumulated when the scattering was unduly influenced by "dust" or other anomalous conditions could be rejected. The effects of possible fluctuations of the laser intensity were minimized by the use of the short-term estimates of the theoretical background. Finally, it was possible to apply a chi-square (χ^2) test to the adequacy of the model selected for $N(R)$ by using the estimates of the experimental variance of $g^{(2)}(\tau, \theta)$.

Error Analysis

The variance associated with the best-fit $N(R)$ that results from the procedures described was estimated as follows. The best-fit values of the s_i are denoted s_{i_0} and the minimum value of χ^2 is χ_0^2. The free fitting parameters $s_i \neq s_f$ were selected one at a time for error evaluation. With the value of s_i fixed at a new value:

$$s_i = s_{i_0}(1 + \delta_i), \tag{9}$$

the other free parameters $s_j (j \neq f, j \neq i)$ were freely varied by the nonlinear least squares program until the best fit with the restriction of Eq. 9, and the corresponding value of $\chi^2(s_i)$ were found. For each $i \neq f$ this procedure was repeated for enough values of δ_i to define the set $\{s_i \mid (\chi^2(s_i) - \chi_0^2) < 1\}$. This set defines the standard deviation associated with s_i(9).

The particle size distribution is presented as a normalized mass density function $M(R)$, easily derived from $N(R)$. The integral of $M(R)$ over all R is 1. This normalization condition couples the parameter fixed in $N(R)$ to the other parameters. Consequently there is a standard deviation associated with each parameter in the mass distribution.

Knot Selection

The fitted $M(R)$ depends to an extent on the set of knots selected. It is possible to utilize an algorithm that, given the number of knots, places these knots at positions that lead to the lowest possible χ^2 (12). This approach was not taken. It would complicate the computations significantly and the quality of the fit is, in fact, quite insensitive to the specific positions of the knots, provided there are enough knots placed near "appropriate" locations. Thus the repeated convergence of a least squares algorithm to a single set of knot positions would be problematic.

---

[1] Fraser, A. Unpublished.

[2] Barenholz, Y., D. Gibbs, B. J. Litman, J. H. Goll, T. E. Thompson, and F. D. Carlson. Manuscript in preparation.

TABLE I

CUMULANT ANALYSIS OF DATA OF FIG. 1

Angle	22.01°	28.81°	61.19°	90.0°	118.81°
$\bar{\Gamma}/q^{2*}$	1.597 ± 0.007	1.633 ± 0.022	1.618 ± 0.006	1.574 ± 0.023	1.571 ± 0.022
Q‡	0.170 ± 0.010	0.166 ± 0.009	0.127 ± 0.008	0.072 ± 0.015	0.111 ± 0.012

*$\bar{\Gamma}$ is the intensity-weighted average of the decay constant $\Gamma = D(R)q^2(\theta)$.

‡Q is the value of $M_2/\bar{\Gamma}^2$ where M_2 is the intensity-weighted average value of $(\Gamma - \bar{\Gamma})^2$.

Knots were restricted to the interval between 90 and 2,000 Å. These limits were based on results of other measurements (15): they could not confidently set by using established light scattering techniques only. The use of such limits considerably reduced the ambiguity in the fitted distributions, especially for small particles. An important advantage of the spline-fitting technique is the ease with which such additional information can be incorporated into the fitted function (7).

Initial fitting utilized 14 knots. The error analysis showed that the 11 associated free parameters were not independent: only 4 or 5 independent parameters could be determined. "Improper" placement of the knots resulted in an increased χ^2. The fitted distribution obtained with excess degrees of freedom was used to determine where knots were necessary when fewer degrees of freedom were used in the fit.

RESULTS AND DISCUSSION

The method was used to analyze PCS data taken using a solution of vesicles composed of 75% egg phosphatidylcholine and 25% egg phosphatidylethanolamine. The results of cumulant analysis are summarized in Table I. Although Γ was linear with q^2 in the range investigated, the "polydispersity index," Q, showed a fairly strong angular dependence, and took on values too high to be accounted for by a monodisperse preparation. Finally, the data showed statistically significant deviations (largest at the lowest angles) from single exponential functions. The sample thus showed some polydispersity, due in part to the presence of non-Rayleigh scatterers.

The data from five scattering angles and the correlation function derived from the best-fit $N(R)$ are illustrated in Fig. 1. The standard deviations of the normalized $g^{(2)}(\tau, \theta)$ range from 0.0019 to 0.0038. The fit is excellent, as indicated by the value, 1.12, of chi-square per degree of freedom (χ^2_ν). Fig. 2 illustrates the best-fit distributions obtained with two different sets of knots. These two distributions give virtually identical fits to the data. The maximum difference between correlation function points derived from the two distributions is less than 0.0004 and the values of χ^2_ν are 1.119 (solid curve in Fig. 2) and 1.128 (dashed curve). The two distributions differ significantly only for $R < 140$ Å. The data are consistent with both of these distributions and various other similar ones as well. It is not possible to resolve this ambiguity by using additional knots: only four of five independent parameters can be defined with reasonably small standard deviations. This result reflects the well-known insensitivity of PCS to localized polydispersity (3). Several important features of the distribution are, however, independent of which set of knots is chosen. The total fraction

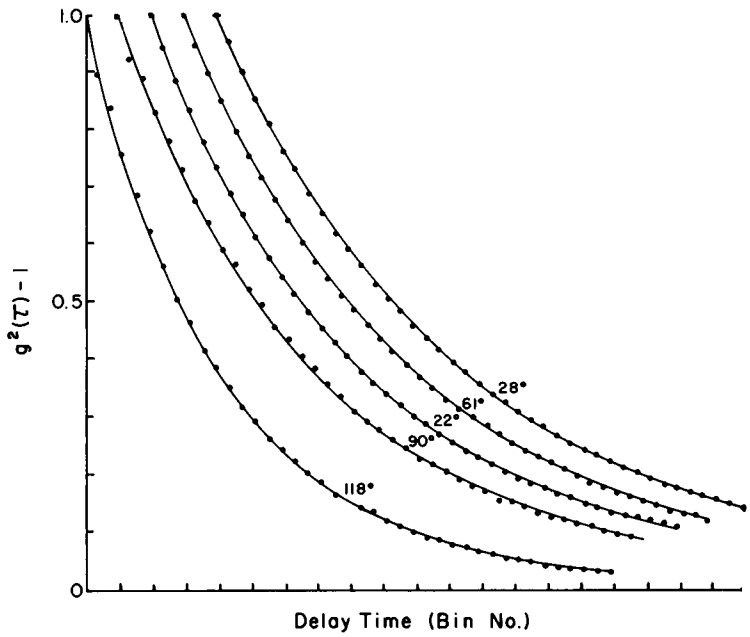

FIGURE 1 PCS data (•) from five angles taken by using a solution of 25% phosphatidylethanolamine: 75% phosphatidylcholine vesicles and fit (——) to the data with best-fit $N(R)$.

of mass (87%) in particles with $R < 140$ Åis the same in both cases illustrated in Fig. 2. The distributions are virtually identical for $R > 140$ Å. In both cases about 13% of the mass is indicated between 140 Å and 300 Å, and much less than 1% is indicated for $R \geq 300$ Å. While the actual percentages might vary somewhat if different knots were selected, it is clear that on the order of 10% of the mass is in particles of intermediate size (140 Å < 300 Å) and very little mass is in large particles (>300 Å). This information would be very difficult to acquire by other light scattering methods. In another paper,[3] size distributions are reported for vesicles of varying phospholipid composition. Highly sensitive comparisons between similar samples are made there by using essentially the same knots for all data. The results for egg phosphatidylcholine vesicles reported there are in excellent agreement with analytical ultracentrifugation results reported by Huang and Lee (16).

The best-fit distributions obtained using a single set of knots and data from low angles only (22° and 28°), from high angles only (61° and 90°), and from all five angles are charted in Table II. The values of the distribution parameters for the three cases fall within one or two standard deviations. Thus the characterization of the distribution does not depend significantly on the scattering angle selected. The standard deviations of the distribution parameters are, however, smallest when all the data are used.

[3]Goll, J. H., Y. Barenholz, B. J. Litman, T. E. Thompson, and F. D. Carlson. Manuscript in preparation.

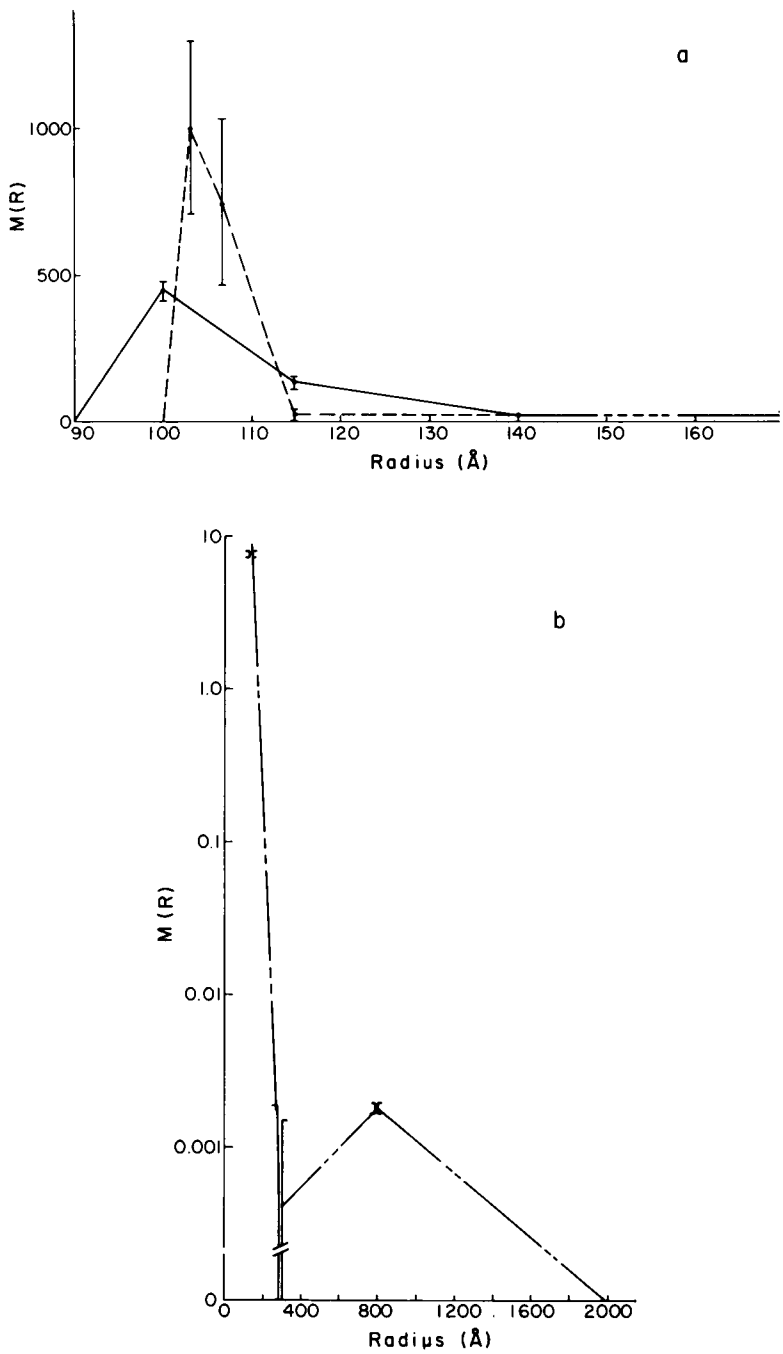

FIGURE 2 Mass density function $M(R)$ for sample of Fig. 1. $M(R)$ is plotted for two different sets of knots: *a*). $R \leq 140$ Å. *b*). $R \geq 140$ Å. The point $R = 140$ Å is common to both diagrams. Note that *b* is plotted semilogarithmically. In *b* the two curves nearly superimpose, and are drawn as one. Error bars (] and [) belong with the dashed and solid curves, respectively.

TABLE II

VALUES OF $M(R)$ FOR SAMPLE OF FIG. 1, USING DATA FROM VARIOUS SETS OF ANGLES

Set of angles	Radius (Å)						
	90	100	115	140	300	800	2,000
22°, 28°, 61° 90° and 118°	0	445 ± 30	130 ± 20	7.5 ± 0.3	0.0008 ± 0.0008	0.00185 ± 0.0001	0
22° and 28°	0	533 ± 125	95 ± 95	5.4 ± 2.2	0.035 ± 0.030	0.0022 ± 0.0006	0
61° and 90°	0	300 ± 60	231 ± 43	6.1 ± 1.1	0.016 ± 0.016	0.0006 ± 0.0006	0

Although χ_ν^2 is ~1 when data from all five angles or only the higher angles are used, it is unreasonably low—0.19—when only the low-angle data are used. This low value of χ_ν^2 probably indicates that in addition to the expected random statistical error there is a correlated error in the low-angle data. (For example, fluctuations in the number of large particles in the scattering volume from one short experiment to the next would lead to a correlated error.) The effects of any correlated errors could be removed if the data from the individual short experiments were available. In this case they are unavailable. Because of this problem, the simultaneous fit to data taken at five angles is not as good as indicated by the apparent value of χ_ν^2. The model of the scattering population used here is thus not quite adequate to describe all the data. It is nevertheless significant that the model comes as close as it does.

Finally, when simultaneously fitting data gathered at several angles, a problem resulted from our inability to gather all the data at the same time. Occasionally low-angle data could not be fit together with data from higher angles. Sometimes this was due to "dust" contributions, which varied from one run to the next. With some samples the problem was systematic, indicating an inability of the model of the scattering population to account for all the data.

The principal advantage of the present method is that it allows considerable flexibility in the fitting function used, and thus in the types of data that can be fit successfully. Furthermore, external constraints (such as the bounds imposed on "allowed" sizes) may be readily incorporated in the model. Finally, specialized distributions such as bimodal or multimodal functions may be used readily in cases when such distributions are anticipated. In general the method described here makes it possible to obtain more detailed results from light scattering experiments by utilizing both extensive PCS data and information about the sample obtained by other means.

The authors are grateful to Prof. F. D. Carlson for his many valuable suggestions and to Dr. Y. Barenholz, Prof. B. J. Litman, and Prof. T. E. Thompson for providing the vesicle solutions and for much helpful discussion.

This work was supported by U.S. Public Health Service grants GM 05181, AM 12803, and AM 16315.

Received for publication 6 August 1976 and in revised form 2 May 1977.

REFERENCES

1. CARLSON, F. D. 1975. The application of intensity fluctuation spectroscopy to molecular biology. *Annu. Rev. Biophys. Bioeng.* **4**:243.
2. PECORA, R. 1972. Quasi-elastic light scattering from macromolecules. *Annu. Rev. Biophys. Bioeng.* **1**: 259.
3. KOPPEL, D. E. 1972. Analysis of macromolecular polydispersity in intensity correlation spectroscopy: the method of cumulants. *J. Chem. Phys.* **57**:4814.
4. PUSEY, P. N. 1973. Measurement of diffusion coefficients of polydisperse solutions by intensity fluctuation spectroscopy. *In* Industrial Polymers Characterization by Molecular Weights. J. E. S. Green, R. Dietz, editors. Transcripta, London, U.K.
5. BARGERON, C. B. 1974. The measurement of a continuous distribution of spherical particles by intensity correlation spectroscopy: analysis by cumulants. *J. Chem. Phys.* **61**:2134.
6. ARAGON, S. R., and R. PECORA. 1976. Theory of dynamic light scattering from polydisperse systems. *J. Chem. Phys.* **64**:2395.
7. STOCK, G. B. 1976. Application of splines to the calculation of bacterial swimming speed distributions. *Biophys. J.* **16**:535.
8. MANDEL, L. 1963. *Prog. Opt.* **2**:183.
9. BEVINGTON, P. R. 1969. Data Reduction and Error Analysis for the Physical Sciences. McGraw-Hill Book Company, New York. 336 pp.
10. VAN HOLDE, K. A. 1971. Physical Biochemistry. Prentice Hall, Inc., Englewood Cliffs, N.J. 246 pp.
11. KERKER, M. 1969. The Scattering of Light and Other Electromagnetic Radiation. Academic Press, Inc., New York. 666 pp.
12. GREVILLE, T. N. E. 1968. Introduction to spline functions. *In* Theory and Applications of Spline Functions. T. Greville, editor. Academic Press, Inc., New York. 1.
13. MARQUARDT, D. W. 1963. An algorithm for least-squares estimation of non-linear parameters. *SIAM (Soc. Ind. Appl. Math.) J. Appl. Math.* **11**:431.
14. CARLSON, F. D., B. BONNER, and A. FRASER. 1972. Intensity fluctuation autocorrelation studies of resting and contracting frog sartorius muscle. *Cold Spring Harbor Symp. Quant. Biol.* **37**:389.
15. HUANG, C., and T. E. THOMPSON. 1974. *Methods Enzymol.* **32**:245.
16. HUANG, C., and L. LEE. 1973. Diffusion studies on phosphatidylcholine vesicles. *J. Am Chem. Soc.* **95**:234.